PSFC/JA-08-40

Wall-Actuated Scanning Probe(WASP) For High-Field Side Plasma Measurements On Alcator C-Mod

Smick, N., LaBombard, B.

December 2008

Plasma Science and Fusion Center
Massachusetts Institute of Technology
Cambridge MA 02139 USA

This work was supported by the U.S. Department of Energy, Coop. Agreement DE-FC02-99ER54512.

Wall-Actuated Scanning Probe (WASP) For High-Field Side Plasma Measurements on Alcator C-Mod

Noah Smick* and Brian LaBombard
Plasma Science and Fusion Center,
Massachusetts Institute of Technology,
Cambridge, Massachusetts 02139
(Dated: December 15, 2008)

A new, high-field side scanning probe has been added to Alcator C-Mod's complement of edge diagnostics. The WASP is designed to provide all the benefits of a linear plunge, multi-electrode scanning probe while working from the confined space of the inner tokamak wall. The drive mechanism is an embedded coil which produces a torque with the ambient toroidal magnetic field when energized, thus allowing the probe to plunge to different pre-programmed depths at different times during a plasma discharge. The probe tip is designed for easy replacement and is presently configured to operate as a modified, high heat-flux 'Gundestrup'-type probe with four tungsten electrodes. The probe has demonstrated the ability to obtain cross-field profiles for electron temperature, density, floating potential and plasma flow information (parallel and perpendicular to B) up to a depth of a few millimiters inside the last-closed flux surface in standard C-Mod discharges. The tungsten-tipped probe has proved very robust and shows little or no damage though it routinely handles surface heat fluxes on the order of 100 MW/m^2 at peak insertion.

PACS numbers: 52.70.Ds, 52.30.-q, 52.55.Fa

I. INTRODUCTION

The high-field side (HFS) of a tokamak has always been a difficult location to operate a scanning probe. The lack of diagnostic ports and limited space makes the design and operation of a probe in this region challenging (see Fig. 1). On Alcator C-Mod, which has a minor radius of 22 cm and only 3 cm between the vacuum vessel and the first wall surface, the problem is even more pronounced. As a result, scrape-off layer (SOL) data at this poloidal location has not been available in the past. A number of interesting observations, including MARFES [1] and strong parallel flows [2, 3] eventually led to the implementation of a rudimentary scanning probe on the HFS in Alcator C-Mod. The inner-wall scanning probe (ISP) [4] consisted of a single electrode swing probe, which was mounted on an electromagnetic coil. When the ISP coil was energized it produced a torque with the toroidal magnetic field of the tokamak, causing it to rotate. The actuated probe swung on an arc through the SOL, just brushing the last closed flux surface (LCFS). Though simple, the ISP provided a large amount of information about the HFS SOL. It had the capability of functioning as a parallel Mach probe, by looking first in one direction along a field line and then in the other direction as it executed its scan. Very high parallel Mach numbers were observed (near Mach 1 in some cases), the direction of which reversed when the magnetic flux surface topology was changed from upper to lower-null dominant. These topology-dependent flows disappeared in well-balanced double null configurations, indicating they were driven by cross-field transport on the low field side [5]. The transport asymmetry hypothesis was supported by the observation of lower levels of fluctuations on the HFS and greatly reduced HFS SOL density in well-balanced double null discharges.

While it is tempting to conclude that the SOL flow picture is well described by the parallel dynamics, it is known that large electric fields can exist in the SOL. The resulting $E \times B$ drifts are just one possible source of significant cross-field flow in a flux surface. Due to the small pitch of the field lines, these perpendicular flows can play a large role in the net poloidal flux of particles and energy. It is therefore desirable to have a measurement of the perpendicular flow component. Measuring perpendicular flows via Mach-probe theories [6–8] requires a probe with multiple electrodes, which the ISP did not offer. Other drawbacks to the single-electrode swing probe design include a fixed plunge depth and a poorly defined ion collection area at full-plunge, limiting the useful data to a few mm outside the LCFS.

II. WALL ACTUATED SCANNING PROBE (WASP)

To address the shortcomings of the ISP, we designed the wall-actuated scanning probe (WASP, Fig. 2). This probe makes use of the successful coil-drive of the ISP but couples the motion into a linear-plunge probe using the parallelogram shown in Fig. 3. This design allows a linear plunge probe to operate in the confined space available on the inner wall. The probe is embedded in one of the standard inner wall tile modules, from which

* *Corresponding author:* nsmick@mit.edu,
MIT Plasma Science and Fusion Center,
NW17-170, 175 Albany St. Cambridge, MA 02139.

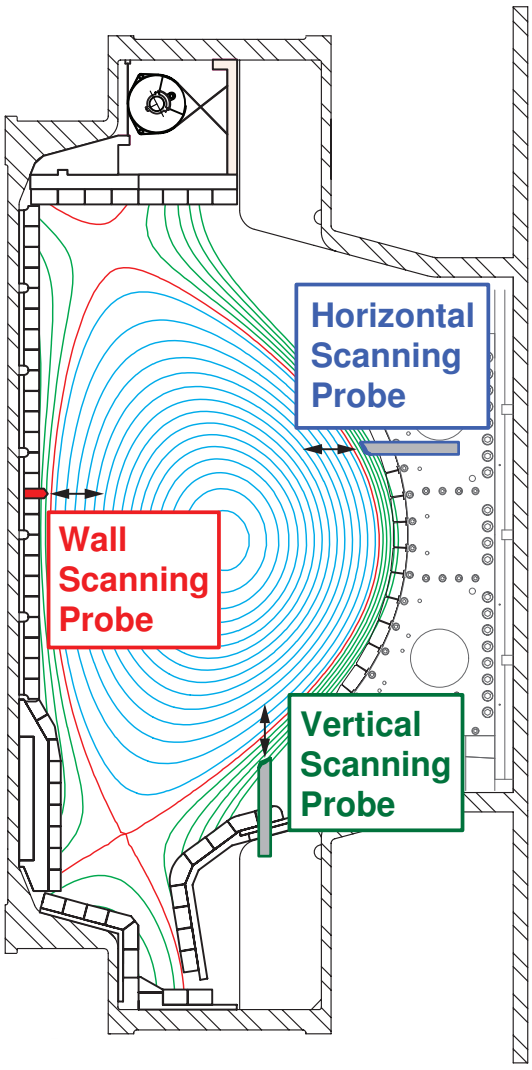

FIG. 1: Cross-section of Alcator C-Mod showing the layout of the scanning probes. Horizontal and vertical scanning probes are activated by linear-motion, pneumatic drives at diagnostic port locations. Lacking port access and physical space, probes at the inner wall location have electro-mechanical actuation.

two of the 16 molybdenum tiles are removed and four more are modified to create the necessary space. The coil moves through an angular range of 0-45°, giving the stage a total linear plunge motion of ∼17 mm, in the major radial direction. The resultant linear range of the probe tip is from roughly -2 mm to 15 mm above the tile surface. The parts of the probe module are described as follows: The tile module, the coil housing, the stage and the probe-tip (see Fig. 2).

A. Pivots and Drive Coil

The idea of using an embedded coil to drive mechanical motion using the ambient toroidal field was first implemented on C-Mod by C.S. Pitcher for the divertor bypass 'flappers' [9] and later used for the ISP [4]. The WASP is the first time such a coil has been mechanically arranged to drive linear motion. As a result, the WASP requires an array of eight pivots which must function in vacuum and survive high temperatures. They must also survive significant mechanical stress due to the inertial forces on the probe and should ideally provide electrical insulation for the probe tip, which should not draw a large current and thus perturb the plasma. The most obvious means of implementing these pivots is to use a shoulder bolt to secure the pivot assembly, but this occupies significant space and has the possibility of the bolt loosening and the probe failing. Since the WASP is inaccessible during a campaign, such a failure is highly undesirable. Our solution was to use compound bushings, which integrate a washer and axle into a single part, wherever possible (see Fig. 4). These bushings are captured in the structure during the assembly of the probe and module. They must endure the shear loads carried by the axle and require superior toughness. For this application, we used zirconia, a ceramic with high fracture resistance. We were able to implement these compound bushings in four of the eight pivot locations, between the stage and coil and between the coil and tile module. The other four pivots were implemented using a stainless steel shoulder-bolt locked against rotation by a set screw, with alumina washers providing electrical insulation and bearing surfaces. All of the ceramic bushings are captured by the structure as much as possible to prevent failure even in the event of a cracked bushing. Embedded torsion springs in two of the shoulder-bolt joints draw the probe back to the wall if it is not energized. This prevents the probe from accidentally being left in an extended position when not in use.

The coil was wound from 28 gauge magnet wire with .025 mm thick polyamide-coating. The coil requires about 10 m of wire and has an inductance of about 50 μH. Its total effective area is roughly .03 m^2. The resistance of the coil is 2.3 Ω. Calculations indicate that the coil can survive being energized at the maximum power supply current of 6 A for 6.5 seconds without melting the polyamide coating. To prevent any shorting of the coil to the metal housing surrounding it, polyamide tape is wrapped around the mandrel of the coil and mica sheets are used to line the sides of the stainless spool. An extra coating of Teflon insulation is placed around the magnet wire where it exits the coil to prevent the coating from abrading over time and shorting the magnet wire to the housing.

B. Stage and Electrode Wires

The molybdenum probe tip extends from the stage. The wiring for the four electrodes is routed through the stage (see Fig. 4). The current from each electrode is carried by a stranded, 28 guage copper wire with a 0.15 mm

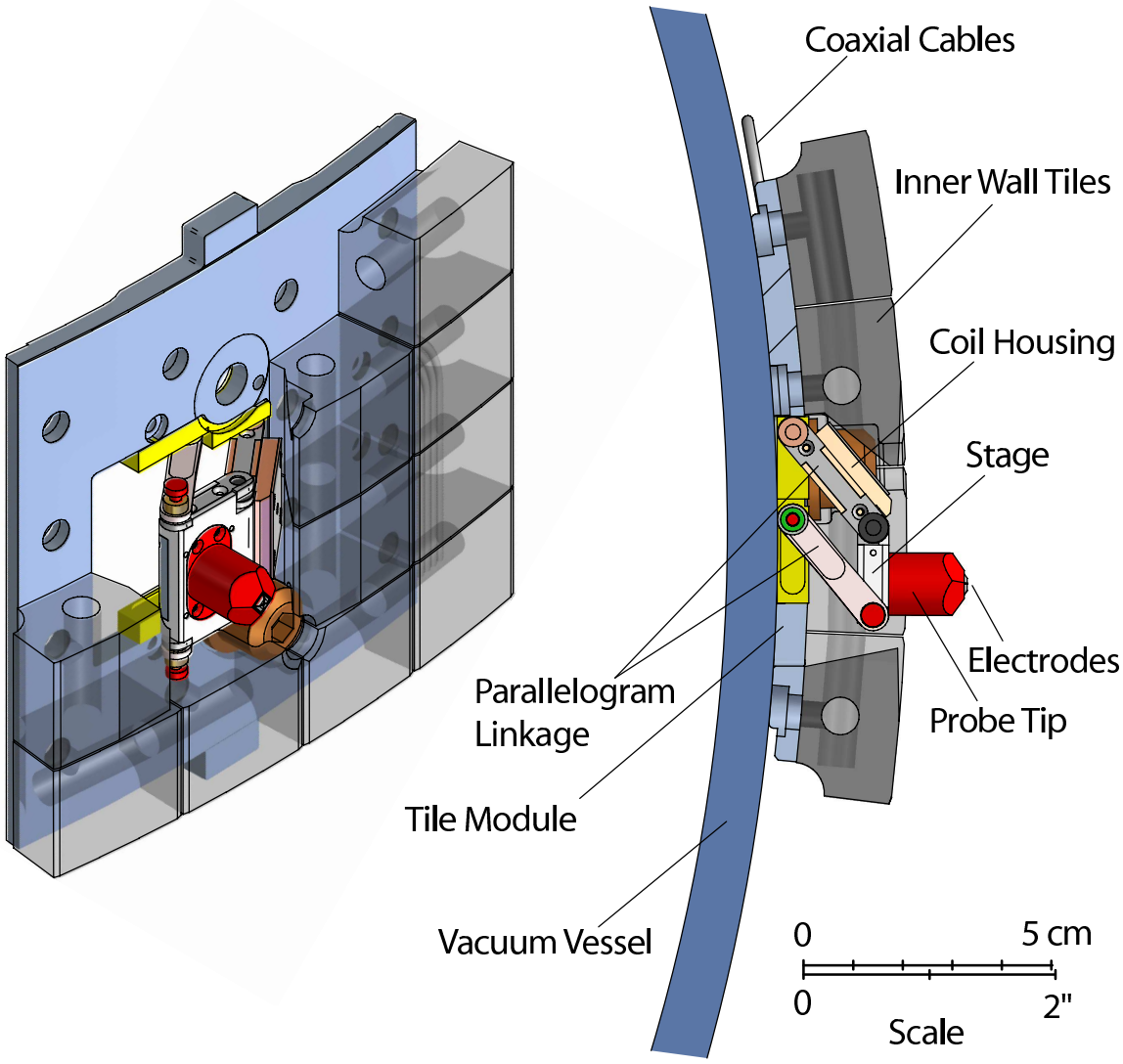

FIG. 2: Wall-actuated scanning probe (WASP) assembly embedded in a C-Mod inner-wall tile module.

Teflon coating. The wire is routed from behind the tile module through the coil housing to the stage. Since the probe tip, and possibly the whole stage are expected to get hot, all electrical insulation in the stage and tip was done with ceramic parts. The electrode wires themselves can heat up both from carrying large currents and thermal conduction from the probe tip, so a ceramic heat sink cradles the wires where they enter the coil body. Further from the plasma, we rely on the wires' Teflon coating for electrical insulation. Calculations indicate that during an event where the probe is exposed to a sufficient heat flux to melt the molybdenum probe tip over 50 ms, the temperature change of end of the wire closest to the electrode would be roughly 85°C. The ohmic heating of the wire is negligible in comparison. This result indicates that in a worst-case scenario, the Teflon ($T_m > 260$°C) is not likely to melt. Furthermore, we have inspected the Teflon after such events and found it intact. Care was taken that there be no direct line of sight from the plasma to the wires as the x-ray and UV light would quickly degrade the Teflon. To this end, shields were created out of shim stock and spot welded onto the coil structure.

There are two points where the wires must bend to follow the motion of the probe. It was feared that these points would be subject to fatigue failure of the wires. The problem is most pronounced at the joint between the coil and stage where the space is the most limited. To mitigate this problem, the wires wrap twice around a rod which is coaxial with the pivot axis. In this way, the wires' bending is distributed over a longer length, minimizing local strain. In addition, the Teflon coating was left on the wires in the area of the pivot even though all of the contact surfaces are ceramic or ceramic-coated. This maintains rigidity of the wire better than free metal strands. For the other pivot, located at the base of the coil, a single turn without a support shaft was used because the additional space reduced the bending requirement on the wires. In the stage, the wires terminate at

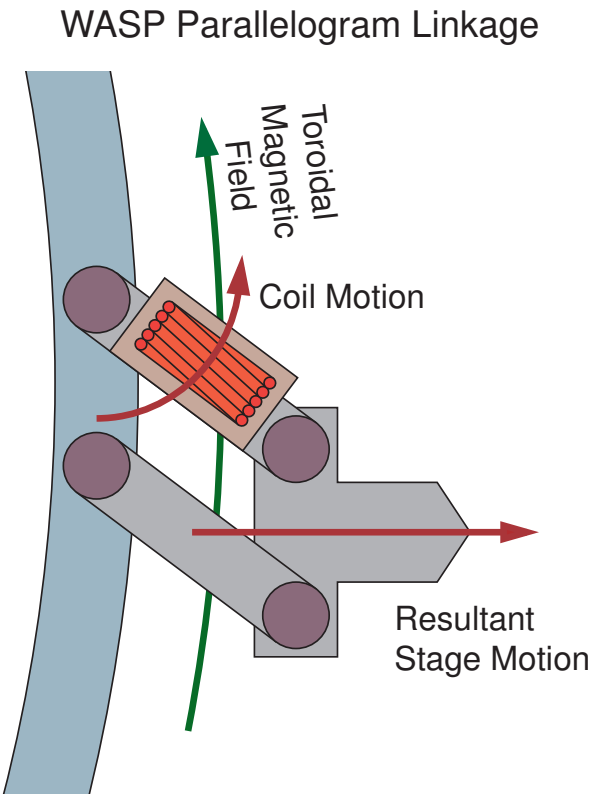

FIG. 3: Illustration of the WASP coil drive linkage: When energized, the coil attempts to align its magnetic moment with the toroidal field. The parallelogram linkage maintains the orientation of the stage and probe tip with respect to the radial direction, reproducing the effect of linear radial motion.

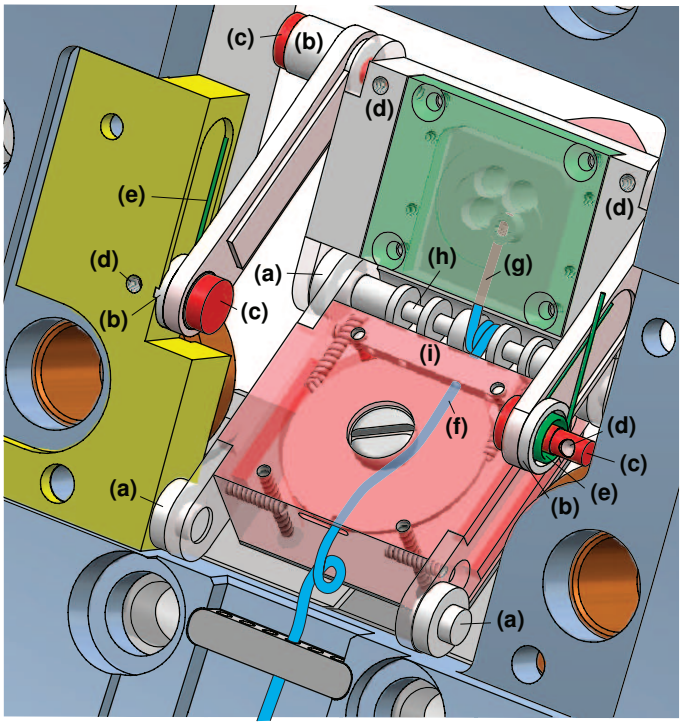

FIG. 4: A back-view of the WASP: (a) 'compound' zirconia bushings, (b) alumina bushings, (c) shoulder bolts, (d) set screws, locking shoulder bolts against rotation, (e) return springs, (f) Teflon-coated electrode wire, (g) uncoated wire, terminating at the base of copper electrode contacts, secured by set screw, (h) alumina wire-support axle, and (i) alumina heat sink. Not shown for clarity: RHS mounting piece, three additional electrode wires and copper contacts, coil wires, limit springs, and small hardware.

the base of the copper spring contacts which connect to the electrodes. They are held in place with a set screw. Behind the tile module, they are connected to co-axial cables with SMA pins.

C. Limit Springs

The motion of the WASP is limited by contact with the wall tiles at the maximum insertion, and contact with the vacuum vessel at maximum retraction. To reduce the inertial forces on the probe when colliding with these stops, finger-spring washers [10] were spot-welded to both the front and back surfaces of the coil housing, and to the back surface of the stage (see Fig. 5). It was at first thought that the springs would be necessary to assist the electro-mechanical drive in turning the probe around quickly at maximum plunge, but we discovered that the EM drive was quite capable of effecting a quick turn-around by itself.

D. Probe Tip

A common failure mode for scanning probes is exposure to excess plasma heat flux. This can happen during a plasma disruption in which control of the plasma is lost and it crashes towards the probe. Over-insertion of the probe can also lead to failure. Both of these events usually result in melting of the surface of the probe tip and the electrodes which then become electrically shorted together. For this reason the probe tip and electrodes are designed so they can be removed easily as a unit and replaced. Four screws hold the probe tip to the stage; they are accessible from the front of the unit. In Fig. 5 they are half-visible behind shim stock which has been spot-welded on the front of the stage to eliminate the possibility of the screws loosening during operation. The electrodes are held in place in the probe tip with a threaded collar, and the electrical connection is made via a spring contact. Inside the stage, the electrode wires terminate in the base of the contacts (see Fig. 4). The wires are held in contact with a set screw. Solder was avoided at this location because we have found that exposure of the ceramic insulators to acid flux can lead to a current

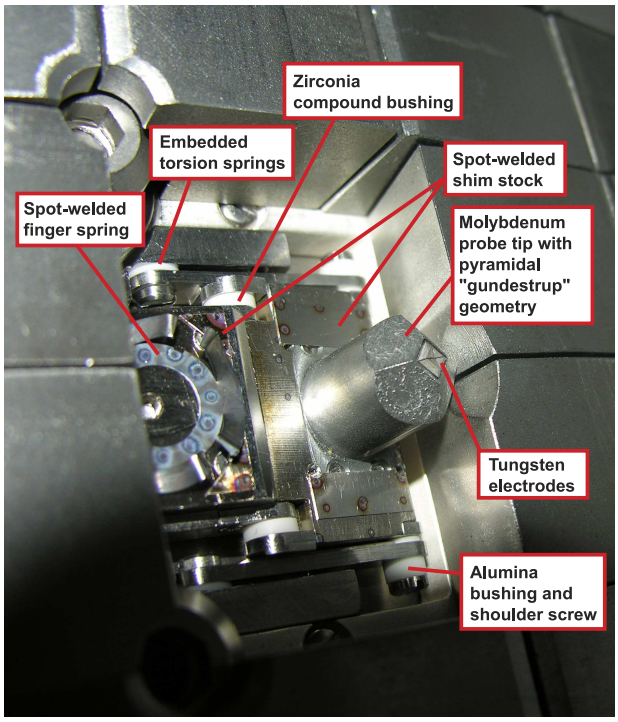

FIG. 5: A WASP probe installed on the C-Mod inner wall.

leakage path between electrodes. However, in retrospect it appears that this may have been the wrong decision. We have experienced occasional open-circuit electrodes during WASP operation which are most likely due to a loosening of the set screw that holds the wires in contact. This could be caused by the repeated motion or repeated thermal cycling of the probe. For future installations, we plan to solder the wires to the connectors, being careful to avoid flux contamination.

The WASP has thus far been outfitted with the new pyramidal Gundestrup probe tip design, which has become the standard for C-Mod scanning probes during the '07 and '08 campaigns. The goal of this four-electrode design is to make use of the fact that the ion saturation current to a facet with a surface normal at an angle to the field is influenced by fluid drifts perpendicular to the field, as well as by plasma flows along the field [6–8]. The use of four facets with angles of 45° to the field (when measured in a flux surface) produces a simplified set of four equations with three unknowns: the density (n), and parallel and perpendicular Mach numbers ($M_{||}, M_{\perp}$) [8] (note: this assumes there is negligable plasma flow in the radial direction).

$$\ln(n_1/n) = M_{||} + M_{\perp} - 1. \tag{1a}$$
$$\ln(n_2/n) = M_{||} - M_{\perp} - 1. \tag{1b}$$
$$\ln(n_3/n) = -M_{||} + M_{\perp} - 1. \tag{1c}$$
$$\ln(n_4/n) = -M_{||} - M_{\perp} - 1. \tag{1d}$$

Here, the electrode numbering is chosen so that the positive $M_{||}$ correspond to electrodes 'looking' in one parallel direction and positive $M_{\perp}$ corresponds to electrodes 'looking' in one perpendicular direction. Also, the 'density' for a given electrode is calculated using the standard form:

$$n_i = \left(\frac{I_s}{qA_p c_s}\right)_i. \tag{2}$$

Where the I_s are the ion saturation currents on the four electrodes, the A_p are the projected areas of the electrodes along the field lines and the c_s are the sound speeds calculated from the local temperature measurements. Eqs. (1) can be solved in a least-squares sense, providing measurements for the three unknowns.

The arrangement of our probe is as follows: four tungsten electrodes are placed at the tip of a molybdenum pyramid that has a steepness of 45 degrees, the altitude of which is in the radial direction, and two edges of which are aligned with the total field (see Fig. 5). The pyramid is at the end of a 12.7 mm diameter shaft. Unlike previous C-Mod probe tip geometries, this design requires the electrodes to be carefully machined to precise geometry, rather than using simple wires which are filed flush with the surface of the probe. The electrodes are machined using EDM and are spray-coated with ∼0.2 mm of alumina, insulating them from the probe body and from each other. The tight group of electrodes placed at the very end of the probe provides high spatial resolution and maximum operational depth.

All four electrodes are normally operated in a swept-voltage mode (2 kHz sweep, -300 to +75 volts maximum bias range with a 2 amp current clamp, see Fig. 6). The current and voltage signals from the electrodes are digitized at 1 MHz. By fitting the positive and negative going $I-V$ characteristics, temperatures and floating potentials can be obtained every .25 ms (corresponding to ∼0.17 mm of probe motion). The waveforms on the four electrodes are programmed by the same voltage waveform generator, so that no large voltage differences occur between them. This reduces the chance for arcing and allows us to place the electrodes closer together. During the period when the probe is biased sufficiently negative to be in the ion saturation regime, the density and flow velocities can be calculated.

This probe geometry can also be used to infer poloidal phase velocity of fluctuations by the time-delay correlation of the ion saturation currents on poloidally adjascent electrodes.

E. Coaxial Cables

The electrical connections to the probe coil and electrodes are made via 50 Ω co-axial cables and feedthroughs, which provide the potential to sample plasma conditions at very high frequency, and to employ advanced signal processing methods such as the mirror

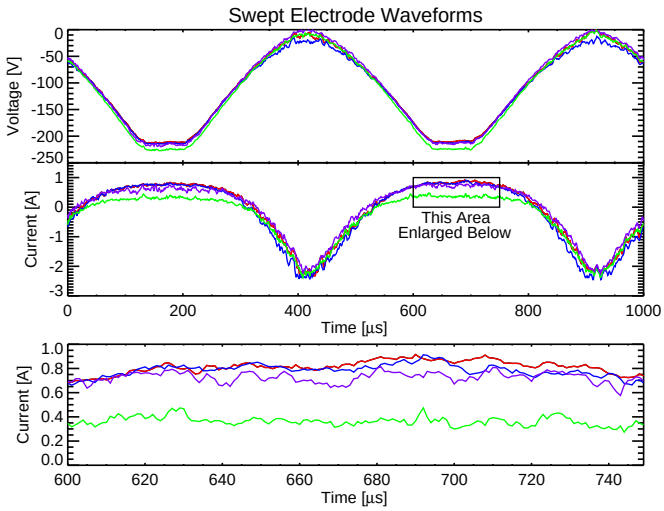

FIG. 6: A 1 ms snapshot of the current and voltage traces from the WASP electrodes. Fitting the I-V characteristic provides density, temperature and floating potential information at 4 kHz. The bottom trace shows the signals from the four electrodes during a period of ion saturation, which are used to extract density and parallel and perpendicular Mach numbers. These signals are digitized at 1 MHz. Time-correlation of fluctuations can provide a measurement of the phase velocity of fluctuations propagating in the perpendicular direction.

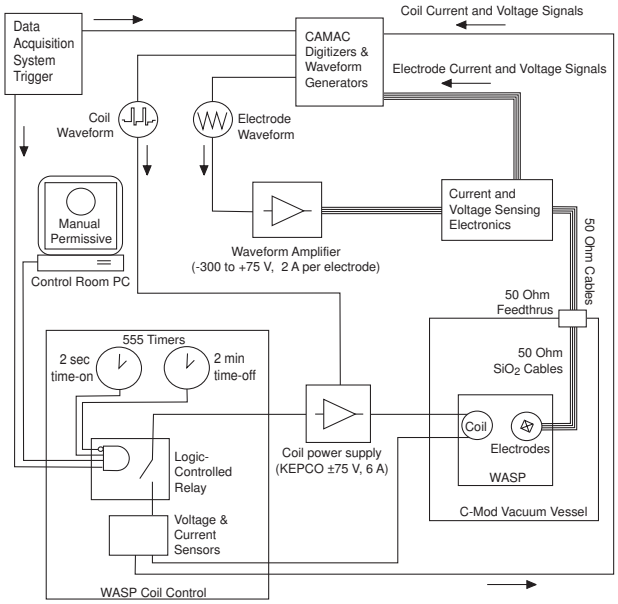

FIG. 7: Block diagram of WASP control electronics and data acquisition system.

Langmuir probe technique [11]. For the invessel sections, we selected a stainless steel jacket, SiO_2 insulated, 2.3 mm diameter cable from Meggitt Safety Systems. The small diameter was necessary due to space limitations behind the inner wall tiles. The 50 Ω cables run to just before the actual probe, leaving only about 70 mm of non-coaxial wire before the electrodes. To allow the entire probe module to be removed without re-routing all the cables, we installed SMA connectors [12] behind the wall tiles.

F. Electronics

The WASP electrodes use the standard set of electronics available to bias and record Langmuir probe data on C-Mod. Additional WASP-specific electronics have been developed to drive the coil (see Fig. 7). These include a series of logical interlocks which require an active shot cycle and a manually set permissive to fire the probe. This allows us to disable the probe independent of the shot cycle, which can be very useful in a panic situation. These interlocks communicate with a relay which connects the coil to its power supply. An anticipated failure mode for the control system was that a large current might be driven for an extended period, potentially melting the coil windings. To avoid this, we employ a pair of 555 timers in the circuit which allow the coil to be energized for only a two-second window and then have it time out for about two minutes. This should never interfere with normal probe operations, but should prevent an over-current failure. The coil current is measured by adding a high-power, high accuracy 1 Ω resistor in series with the coil and measuring the voltage across it. (Note that this resistance is included in the R in Eq. (4)). The voltage and current signals are monitored via high-impedance op-amps and sent to CAMAC digitizers.

III. ELECTRO-MECHANICAL MODEL

The WASP coil drive is based on those that were used for the ISP [4] and divertor bypass flappers [9]. The torque balance on the probe assembly is given by:

$$I_m \frac{d^2\theta}{dt^2} = \tau_{coil} + \tau_{spring} + \tau_{eddy}$$
$$= AIBcos\theta - k(\theta - \theta_0) - \kappa B^2 cos^2\theta \frac{d\theta}{dt}. \quad (3)$$

Where I_m is the effective moment of inertia of the probe assembly, θ is the angle of the coil from its rest position, A is the effective area of the coil, I is the current driven in the coil, B is the magnetic field, k is the spring constant of the return springs, θ_0 is the rest angle of the return springs, and κ is an eddy current coefficient. It must be recognized that this model is inaccurate in that it assumes the object is a rigid rotor, which is not the case for the WASP. We would expect both κ and I_m to vary with θ due to the changing geometry as the coil rotates. A careful calculation of the moment of inertia shows that it varies by only about 6% over the coil's range of motion. The primary challenge in making an accurate model is correctly calculating the magnitude of the eddy currents

induced in the probe as a result of its motion. These effectively set a terminal velocity for the probe. Because of the strong impact that this has on the dynamics of the probe scan, and in particular the amount of time it would spend in the plasma, it was decided that we should test the WASP off-line in a high field environment. This would also give us the opportunity to evaluate the mechanical durability of the design.

To perform these tests, we made use of the 1-J Magnet, operated by the PTF group at the MIT Plasma Science and Fusion Center. This water-cooled copper magnet can achieve magnetic fields as high as 4.5 Tesla for a few seconds, providing us a dataset that we could extrapolate to the 5-12 Tesla typically found at the inner wall of Alcator C-Mod. At the time of the test, we did not yet have the ceramic bearings available, so we used a set of graphite bearings instead. The probe was outfitted with mechanical limit switches which could sense if the probe was at maximum plunge or if it was fully retracted. These data supplemented the results of the back-EMF integration, which is the means of measuring the probe position when it is operated on C-Mod. The back-EMF is calculated using the equation:

$$V = IR + ABcos\theta\frac{d\theta}{dt} + L\frac{dI}{dt}. \qquad (4)$$

The self-inductance term (last term) has minimal effect on the result because the field generated by the coil is always much less than the ambient field in the tokamak. The only time it could be important is when the current is rapidly changed in the coil (e.g., at maximum plunge when the polarity is reversed) but we find experimentally that including this term makes very little difference in the result. Therefore only a rough measurement of the coil inductance is required. It should also be noted that by solving this equation, one implicitly assumes that R and B have no time dependence. This is generally well satisfied, but care must be taken in the case of a rapidly ramping field. Given steady R, B and small L we need only know the effective area of the coil and its resistance to calculate the trajectory of the WASP from the coil $I-V$ characteristic. A robust method of calculating the resistance is to apply a small reverse voltage to the coil throughout the shot which holds the coil firmly against the wall (see Fig. 9). The current passed in the stationary coil is used to measure the resistance before and after each scan to provide a nearly continuous calibration, which can track changes in the resistance due to changing coil temperature. The effective area can then be calibrated by comparing the back-EMF output to the known range of motion of the WASP.

We conducted WASP tests using the 1-J Magnet over a period of two days. The back-EMF integration and the signals from the limit switches confirmed that the probe was able to scan through its entire range and back in a time of ∼30 ms. This was less than the 50 ms scan time of the ISP, minimizing the probe's dwell time in the plasma. We collected data at a variety of magnetic fields ranging from 1 to 4.5 Tesla. This allowed us to fit the data to a computer model of the probe motion based on Eq. (3). We were then able to extract various constants which could be used to predict the motion of the probe in C-Mod. Several traces of predicted motion compared to observed motion are shown in Fig. 8. Note that our model does not account for energy dissipation in the collision of the probe with the wall (which appears to be substantial) or in friction in the bearings. However, it is fairly accurate in predicting the free motion of the probe. While the model is not needed for the normal operation of the WASP, it can be helpful in predicting the response of the coil drive to new magnetic field conditions or new driving waveforms, which can be more convenient and less hazardous than a trial-and-error approach.

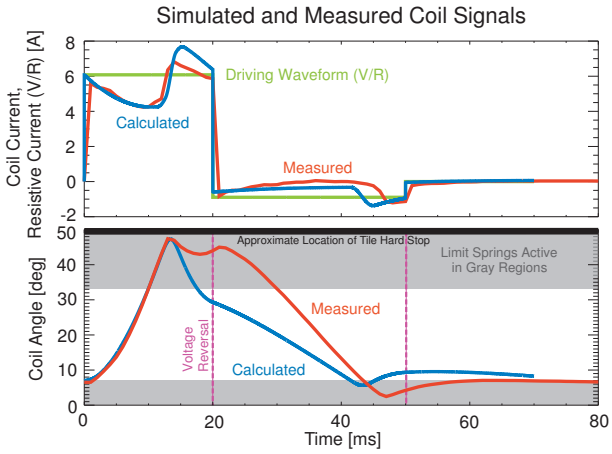

FIG. 8: The model which predicts the coil motion can be used to roughly anticipate the response of the coil-drive to different field conditions and driving waveforms. The plunge depth measured by integrating the coil back-EMF provides the radial position measurements we report with our data.

While testing the WASP on the 1-J magnet, we scanned the probe many times during a magnet pulse to evaluate its durability. A total of 100 scans were performed on the first day of testing, 400 on the second. Two of the graphite bearings fractured during the test, but this did not inhibit the operation of the probe. It did however confirm our suspicions that graphite would be an insufficient structural material for the bearings, motivating our use of ceramics. It is worth noting that very low fields result in more violent motions of the probe since the damping due to eddy currents is reduced. In the end we were satisfied that the probe would be sufficiently durable to survive operations inside C-Mod.

IV. WASP OPERATION

The WASP probe was operated for the first time in the spring of 2007. It was first tested during no-plasma, toroidal-field-only pulses at the beginning of the cam-

paign. This allowed us to verify that the probes were scanning and our back-EMF plunge calculation was functioning as expected. Throughout the '07 and '08 campaigns we operated the WASP without any problems affecting the coil drive or structural integrity. As mentioned before, we did struggle with some intermittent open circuit problems on the electrode due to an electrical connection that was made with a set screw. For the next campaign, we plan to solder this connection.

On two occasions, we melted a probe tip. Once was due to an operator error: setting the plunge too deep. The other was the result of a disruption induced by another scanning probe plunging too deep. During the up-to-air between the '07 and '08 campains, we replaced the probe tip while the WASP coil and stage remained installed on the inner wall, a procedure that was quick and easy, as expected.

The WASP's EM drive affords us the ability to auto-target the probe based on the results of a previous shot. Using an identical program to control the magnetic flux surface shape and location of the plasma, we can reasonably expect the position of the LCFS to follow a similar trajectory in time. The WASP has the ability to plunge to any specified depth depending on what driving waveform is used in the coil. This means that on identical shots, a program can be written that targets the exact depth of the separatrix (or any specified flux surface) independently for several pulses at several different times (see Fig. 9 for an example). This is an extremely useful operational feature which removes all the anxiety and guess-work from the targeting process and greatly improves the efficiency of our experiments. This system was implemented for the WASP based on empirical measurements of the probe response to a variety of driving waveforms in a variety of fields. It typically hits its target to within ± 1 mm.

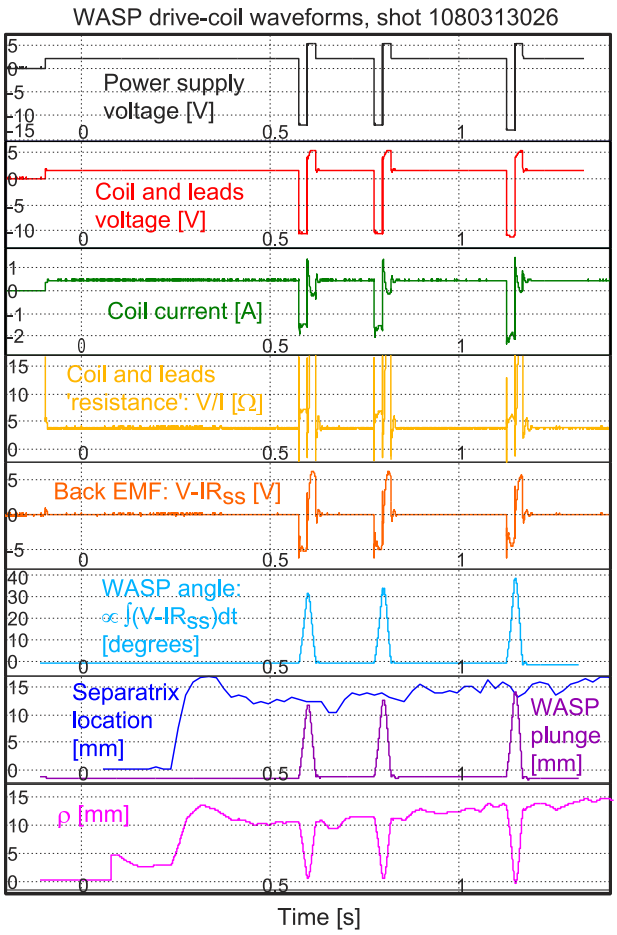

FIG. 9: Typical waveforms for the WASP coil drive during a C-Mod discharge. Note that the 'resistance' calculated by V/R has a steady value between plunges when the coil is held against the wall with a reversed voltage. During this time, the coil is stationary and the current is constant. This provides the value of R_{ss} which is used in the back-EMF calculation. The final result, ρ, is the position of the probe in the SOL measured from the LCFS.

V. SAMPLE RESULTS

Some sample data obtained with the WASP is shown in Fig. 10 with the horizontal and vertical probe data included for reference. All three of these probes were operating with the 'pyramidal Gundestrup' probe tip described in section II D. The smooth curves shown are a spline fit to the data points. The plasma heat flux flowing parallel to magnetic field lines is shown for this typical case, but the probe routinely handles parallel heat fluxes in excess of 600 MW/m^2 at peak insertion.

Note that the WASP data agrees well with the other scanning probes, with the exception of the parallel Mach number, which we believe to be indicative of a transport-driven parallel flow pattern [5]. This pattern is characterized by a ballooning-like poloidal transport asymmetry which populates the LFS SOL with particles. The resulting parallel pressure gradient drives strong flows toward the HFS divertor. This means that the HFS flow velocities are determined almost exclusively by magnetic flux surface topology and plasma density, while other physics seems to play a dominant role in parallel flow dynamics on the LFS. The perpendicular flow velocity often shows a shear layer in the vicinity of the separatrix. This phenomenon is still under investigation; in particular we are trying to determine the relative contributions of $E \times B$ and diamagnetic drifts to the measurement. Recent work by Hutchinson addresses this question [8].

VI. SUMMARY

A new scanning probe, the WASP, has been designed and installed on the high-field side of the Alcator C-Mod Tokamak. Its linear-plunge, multi-electrode design provides all the capabilities of the pneumatic scanning probes routinely operated on the low field side of C-Mod. The WASP's electro-mechanical drive mechanism

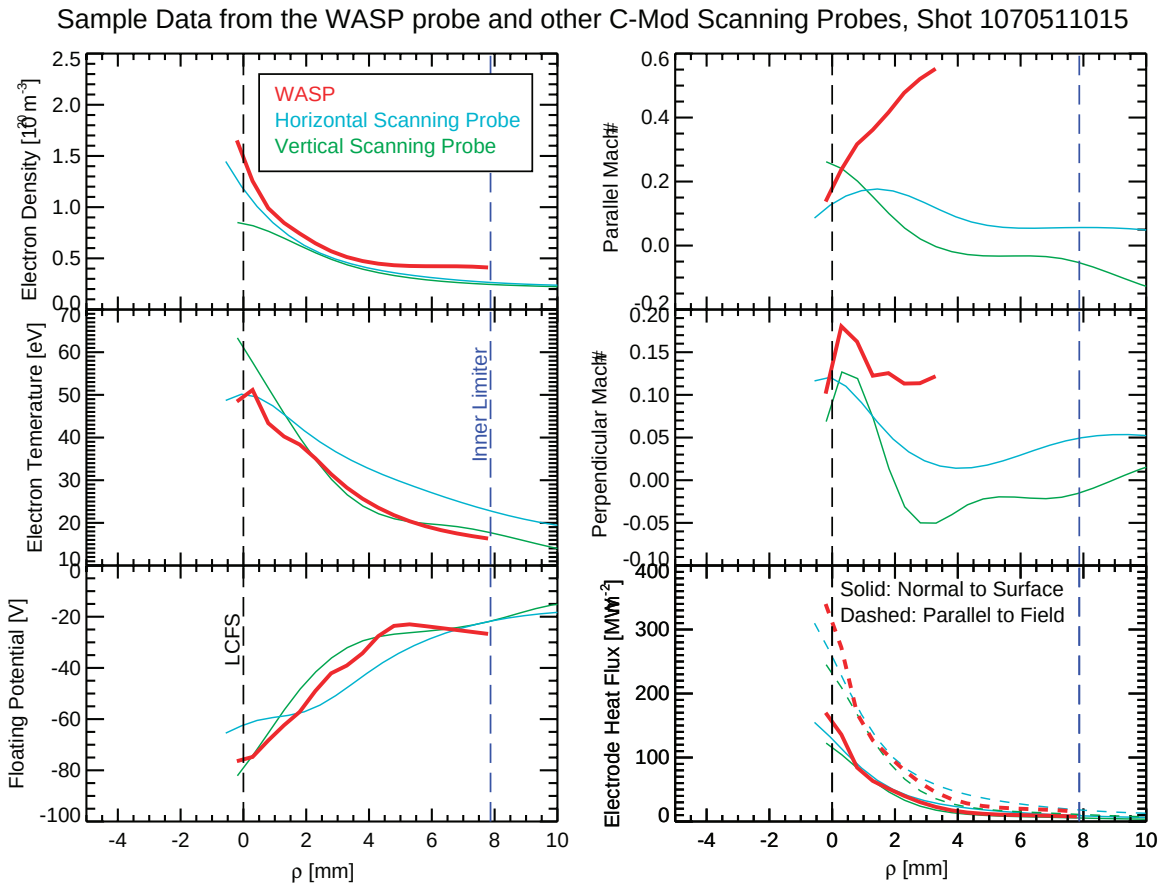

FIG. 10: Sample WASP data Compared with Other Scanning Probes.

provides a high degree of operational flexibility, as well as the ability to calculate the probe position without direct instrumentation. The probe has been operated for the '07 and '08 campaigns and has been successful in measuring density, temperature, potential and parallel and perpendicular Mach number of the scrape-off layer plasma near the inner wall.

[1] Lipschultz, B., Terry, J.L., Boswell, C., Hubbard, A., LaBombard, B., and Pappas, D.A., Phys. Rev. Lett. **81** (1998) 1007.

[2] Jablonski, D., LaBombard, B., McCracken, G.M., Lisgo, S., Lipschultz, B., Hutchinson, I.H., Terry, J., and Stangeby, P.C., J. Nucl. Mater. **241 – 243** (1997) 782.

[3] LaBombard, B., Goetz, J.A., Hutchinson, I., Jablonski, D., Kesner, J., Kurz, C., Lipschultz, B., McCracken, G.M., Niemczewski, A., Terry, J., Allen, A., Boivin, R.L., Bombarda, F., Bonoli, P., Christensen, C., Fiore, C., Garnier, D., Golovato, S., Granetz, R., Greenwald, M., Horne, S., Hubbard, A., Irby, J., Lo, D., Lumma, D., Marmar, E., May, M., Mazurenko, A., Nachtrieb, R., Ohkawa, H., O'Shea, P., Porkolab, N., Reardon, J., Rice, J., Rost, J., Schachter, J., Snipes, J., Sorci, J., Stek, P., Takase, y., Want, Y., Watterson, R., Weaver, J., Welch, B., and Wolfe, S., J. Nucl. Mater. **241 – 243** (1997) 149.

[4] Smick, N., LaBombard, B., and Pticher, C.S., J. Nucl. Mater. **337 – 339** (2005) 281.

[5] Labombard, B., Rice, J.E., Hubbard, A.E., Hughes, J.W., Greenwald, M., Irby, J.H., Lin, Y., Lipschultz, B., Marmar, E.S., Smick, N., Wolfe, S.M., and Wukitch, S.J., Nucl. Fusion **44** (2004) 1047.

[6] Chodura, R., Phys. Fluids **25** (1982) 1628.

[7] Van Goubergen, H., Weynants, R.R., Jachminch, S., Van Schoor, M., Van Oost, G., and Desoppere, E., Plasma Phys. Control. Fusion **41** (1999) L17-L22.

[8] Hutchinson, I.H., Submitted to Phys. of Plasmas (2008).

[9] Pitcher, C.S., LaBombard, B., Danforth, R., Pina, W., Silveira, M., and Parkin, B., Rev. Sci. Instrum. **72** (2001) 103.

[10] Spec Finger Spring Washers: model numbers F0595-010, F0728-006.

[11] Labombard, B., and Lyons, L., Rev. Sci. Instrum. **78** (2007) 073501.

[12] Huber and Suhner SMA connecters: model numbers 11SMA-50-2-65/119NE, 21SMA-50-2-15/111NE.